

Title:

1
2 Population-Based Design of Mandibular Fixation Plates with Bone Quality and Morphology
3
4
5 Considerations
6
7
8

9
10 **Abbreviated Title**

11
12 Population-Based Design of Mandibular Plates
13
14
15
16

17 **Authors:**

18
19 Habib Bousleiman¹
20

21
22 Tateyuki Iizuka³
23

24
25 Lutz-Peter Nolte¹
26

27
28 Mauricio Reyes¹
29
30

31 **Affiliations:**

32
33
34 1. Institute for Surgical Technology and Biomechanics, University of Bern,
35
36 Stauffacherstrasse 78, 3014 Bern, Switzerland
37
38

39 2. Department of Cranio- Maxillofacial Surgery, University of Bern, Inselspital, 3010 Bern,
40
41 Switzerland
42
43
44
45

46 **Corresponding Author:**

47
48 Habib Bousleiman
49

50
51 Phone: +41 (0) 31 631 59 48
52

53
54 Facsimile: +41 (0) 31 631 59 60
55

56
57 e-mail: habib.bousleiman@istb.unibe.ch
58
59
60
61
62

Abstract:

1
2 In this paper we present a new population-based implant design methodology, which
3
4 advances the state-of-the-art approaches by combining shape and bone quality information
5
6 into the design strategy. The method may enhance the mechanical stability of the fixation and
7
8 reduces the intra-operative in-plane bending which might impede the functionality of the
9
10 locking mechanism. The computational method is presented for the case of mandibular
11
12 locking fixation plates, where the mandibular angle and the bone quality at screw locations
13
14 are taken into account. The method automatically derives the mandibular angle and the bone
15
16 thickness and intensity values at the path of every screw from a set of computed tomography
17
18 images. An optimization strategy is then used to optimize the two parameters of plate angle
19
20 and screw position. The method was applied to two populations of different genders. Results
21
22 for the new design are presented along with a comparison with a commercially available
23
24 mandibular locking fixation plate (MODUS[®] TriLock[®] 2.0/2.3/2.5, Medartis AG, Basel,
25
26 Switzerland. The proposed designs resulted in a statistically significant improvement in the
27
28 available bone thickness when compared to the standard plate. There is a higher probability
29
30 that the proposed implants cover areas of thicker cortical bone without compromising the
31
32 bone mineral density around the screws. The obtained results allowed us to conclude that an
33
34 angle and screw separation of 129° and 9mm for females and 121° and 10mm for males are
35
36 more suitable designs than the commercially available 120° and 9mm.
37
38
39
40
41
42
43
44
45
46
47

Key Terms

48
49 Orthopedic implant design, population-based analysis, computational anatomy, mandibular
50
51 locking fixation plate
52
53
54
55
56
57
58
59
60
61
62
63
64
65

Abbreviations, Symbols, and Terminology

1		
2	CT	Computed tomography
3		
4	d	Distance between adjacent screw holes
5		
6		
7	DVF	Deformation vector field
8		
9	f	Objective function
10		
11	H	Local voxel Intensity
12		
13		
14	I	Intensity value
15		
16		
17	n	Number of sampled voxels along one screw path
18		
19	N_r	Number of screws in one region
20		
21		
22	p	Number of image datasets
23		
24	r	Specific anatomical region
25		
26		
27	R	Set of anatomical regions
28		
29	T	Local bone thickness
30		
31	α	Plate angle – mandibular or gonial angle
32		
33		
34	θ	Bone thickness
35		
36	ω_θ, ω_I	Weighting factors
37		
38		
39		
40		
41		
42		
43		
44		
45		
46		
47		
48		
49		
50		
51		
52		
53		
54		
55		
56		
57		
58		
59		
60		
61		
62		
63		
64		
65		

Introduction

1
2 The human mandible is a complex structure and a site of high incidence of traumatic or
3
4 pathologic defects. Reconstruction of defects of the mandible using internal fixators is a
5
6 common procedure in the general and specialized orthopedic wards. Similar to other sites,
7
8 mandibular fixation plates are selected from a limited range of models provided by the
9
10 manufacturers.¹ Therefore the need to intra-operatively adapt the implant to the patient-
11
12 specific anatomy is almost always present, a delicate and time-consuming procedure that is
13
14 prone to high inaccuracies.²
15
16
17
18
19
20

21
22 Manufacturing of internal fixators could range from the entirely patient-specific designs to
23
24 the development of a universal set of implants from which the surgeon selects the most
25
26 suitable on a case-by-case basis. The former type is burdened with increased manufacturing
27
28 and logistic costs, whereas the latter requires careful and sometimes excessive intra-operative
29
30 adaptation to fit the implant to the anatomy of the patient being operated. A tradeoff lies in
31
32 between the two extremes, the so-called population-based design. Current trends tend to pre-
33
34 contour the implants to the average anatomy of the target population or to a template bone
35
36 considered as representative of that population.^{3,4,5} This approach, together with the
37
38 development of locked internal fixators, reduced the need for plate bending.^{3,5,6,7} However, in
39
40 this design approach manufacturers tend to use small populations of cadaveric bones whose
41
42 morphology does not necessarily reflect the actual differences in populations of patients.⁴
43
44 Moreover, it has been shown to be suboptimal when fit criteria besides bone morphology and
45
46 surface-to-surface distances are considered.^{8,9}
47
48
49
50
51
52
53
54
55

56 Recent research presented population-based methods to improve the design of the shape of
57
58 pre-contoured fixation plates.^{8,9} In Kozic *et al.*⁹, an alteration of a commercially available
59
60
61
62
63
64
65

1 proximal tibial implant was proposed based on optimization of surface distances using level-
2 set segmentation in a statistical shape space. In Bou-Sleiman *et al.*⁸, an articulated model of
3 the implant was used to minimize more clinically relevant metrics, namely the amount of
4 bending and torquing required to adapt the implant to the anatomy of the patient undergoing
5 the surgery (as opposed to minimizing surface distances). However, neither one of the
6 approaches incorporates bone quality information into the design. Moreover, they both focus
7 on the out-of-plane deformations and do not address the in-plane bending of the plates.
8
9
10
11
12
13
14
15
16
17
18

19 For the specific case of locking mandibular plates, in-plane bending is the most important
20 type of deformation since it affects the shape of the screw holes and locking mechanism. Out-
21 of-plane deformations are less important in this case because mandibular plates are relatively
22 thin and hence easy to adapt to the patient anatomy. Therefore, for mandibular plates the
23 angle between the mandibular body and ramus, referred to hereafter as mandibular or gonial
24 angle, is of major importance.
25
26
27
28
29
30
31
32
33
34
35

36 In addition to the surface morphology, the mechanical properties of bone are a major criterion
37 to be considered while designing implants,¹⁰ especially in structures such as the mandible
38 where the amount of bone is not in large supply. A well designed implant must present
39 reduced risk of screw pullout and higher mechanical stability. Bone thickness and bone
40 mineral density can be inferred from computed tomography (CT) images where bone
41 porosity, bone density, and image intensity values are well correlated.^{11,12} Moreover, it has
42 been shown that the quality of cortical bone has a considerable positive influence on the
43 stability of the implant.¹³ For the particular case of the mandibular reconstruction plate, the
44 AO Foundation (Davos, Switzerland) recommends flushing the implant to the inferior edge
45
46
47
48
49
50
51
52
53
54
55
56
57
58
59
60
61
62
63
64
65

1 of the body and posterior edge of the ramus. These regions are almost entirely composed of
2 cortical bone.
3

4
5
6
7 In this paper we present a computational population-based design methodology of orthopedic
8
9
10
11
12
13
14
15
16
17
18
19
20
21
22
23
24
25
26
27
28
29
30
31
32
33
34
35
36
37
38
39
40
41
42
43
44
45
46
47
48
49
50
51
52
53
54
55
56
57
58
59
60
61
62
63
64
65

In this paper we present a computational population-based design methodology of orthopedic fixators, which advances the state-of-the-art approaches by combining shape and bone quality information into the design strategy. The proposed methodology is presented for the specific case of mandibular locking plates. Of special interest are the in-plane pre-contouring and the bone thickness and intensity values at screw insertion sites. The implant parameters that we optimize are the plate angle and the distance between adjacent screw holes. In addition we present a comparison between the proposed design and a commercially available model. This paper is an extension of our previous preliminary work¹⁴ where we presented the same method but with certain limitations. Our experimental dataset was limited in size and resolution and we did not consider differences in the anatomy between different genders.

In this study, we assume that there are potential morphological differences between males and females.^{15,16,17} We also assume that the differences between gender groups would lead to different implant designs. Therefore, we separate the available population by gender and apply the design process on each group independently. We also use the obtained results to validate our assumption of gender differences. Furthermore, we apply the method on a larger number of high-resolution CT datasets.

HERE GOES FIGURE 1

Methods

Experimental Data and Pre-Processing

1
2
3
4
5 A total of 80 CT images of the adult skull where the mandibles were manually segmented
6
7 was used in this study. The CT images were acquired at different medical centers with
8
9 varying machine settings. They were originally acquired for diagnostic purposes. Therefore
10
11 the approval of an ethics committee was not required. All patients signed an informed
12
13 consent stating that the data might be used for future research. Anonymity of the datasets was
14
15 observed. The age and gender distributions of the population are listed in Table 1. Each
16
17 image is composed of 193x351x329 voxels and a voxel spacing of 0.4mm.
18
19
20
21
22
23

24 All images were initially rigidly aligned and resampled to the resolution specified above.
25
26 Non-rigid registration was then applied in order to establish a voxel-wise correspondence
27
28 between every image and a predefined reference. The populations were treated similarly and
29
30 independently. Therefore two reference images were selected, one from the male and one
31
32 from the female populations. We used the non-rigid registration algorithm described in Seiler
33
34 *et al.*¹⁸ which was initially presented for mandibles and with a final aim towards implant
35
36 design. The choice of the reference images is considered as integral part of the registration
37
38 process and a pre-requisite to the method we present in this article. The algorithm applies
39
40 local affine transformations onto subdivisions of the original anatomy. This is particularly
41
42 beneficial for the registration of mandibles as it breaks down the complex morphology into
43
44 simpler independent elements. The algorithm yields a deformation vector field (DVF) for
45
46 every image relating voxels in the image to those in the reference via an anatomically
47
48 meaningful correspondence.
49
50
51
52
53
54
55
56
57
58
59
60
61
62
63
64
65

Measurement of the Gonial Angle

1
2 A well-designed plate angle reduces the need of intra-operative in-plane bending and hence
3
4 the risk of deforming the locking screw holes. In order to highlight possible differences
5
6 among the gender-specific populations and to acquire an initial angle value for the angle
7
8 optimization process, we measured the mandibular angle within the set of images in our
9
10 database.
11
12

13
14
15
16 In order to digitally measure the mandibular angle, we manually placed a set of four
17
18 landmark points on the reference mandible. Two landmarks were aligned with the left
19
20 posterior edge of the ramus and the other two were aligned with the left inferior edge of the
21
22 body of the mandible. We used the computed DVF to propagate the coordinates of the
23
24 landmarks to all other images in the population. For every instance, the angle formed between
25
26 the line connecting the two ramal landmarks and that connecting the landmarks on the
27
28 mandibular body was automatically calculated. Fig. 1A illustrates this process graphically.
29
30
31
32

Measurement of Bone Thickness and Intensity Values

33
34
35
36 Similarly, we placed a set of eight landmarks at the screw entry points on the reference
37
38 image. This is analogous to the eight screw holes in the standard plate and consistent with the
39
40 AO guidelines stating that at least three screws must be placed on either side of the fracture.
41
42 We also placed a corresponding set of landmarks on the interior side of the mandible to
43
44 delineate the paths of the screws.
45
46
47
48
49
50

51
52
53 For any particular combination of implant parameters (plate angle and distance between
54
55 adjacent holes), the landmark configuration is modified accordingly and propagated to all
56
57 instances of the population using the computed DVF. Geometrical constraints were integrated
58
59
60
61
62

1 in the computation in order to ensure that the screw holes remain equidistant, that they are not
2 misaligned, and that the plate angle is not affected by the varying mandibular angle due to
3
4 DVF propagation. Additionally, a safety margin of 3mm (consistent with the implant
5
6 dimensions) was set around the screws in order to prevent any parts of the implant from being
7
8 placed outside the bone.
9
10

11
12 The Euclidean distance between each pair of corresponding landmarks was computed. This
13
14 represents the bone thickness at that particular screw insertion site. A 2mm tube (diameter of
15
16 a typical mandibular screws) was used to sample voxels between each pair of landmarks. The
17
18 average intensity value computed along the sampled volume was used to represent the
19
20 cortical bone quality at that location. Fig. 2 shows a 3D view of the landmark configuration
21
22 and the sampled volumes.
23
24
25
26
27
28
29
30

31 **HERE GOES FIGURE 2**

32 *Anatomical Grouping*

33
34
35
36
37
38 Based on recommendations of the AO Foundation and standards of anatomy, the plate and
39
40 mandible were divided into three anatomically distinct regions, namely, the ramus, the angle,
41
42 and the body of the mandible. The regions contain three, two, and three screw holes,
43
44 respectively. Each region was treated separately and considered as a single unit during the
45
46 optimization process and the analysis of the results. The two screws of the angle region were
47
48 used to anchor the plate in place and remain fixed during the optimization. Therefore,
49
50 changes in intensity values or bone thickness are not expected for that region. The
51
52 configuration of the anatomical regions is illustrated in Fig. 1B.
53
54
55
56
57
58
59
60
61
62
63
64
65

HERE GOES TABLE 1*The Design Process*

The mandibular plate was parameterized using two geometric features, in particular the plate angle α and the distance separating two adjacent screws d . The design criteria were the bone thickness and the intensity values per anatomical region $R = \{Ramus, Angle, Body\}$.

For every image in the database, the algorithm scans through the two-dimensional search space and for every pair of parameters computes the intermediate objective function

$$f(\alpha, d)_{im} = \omega_{\theta} \sum_{r \in R} \theta_r^{\alpha, d} + \omega_I \sum_{r \in R} I_r^{\alpha, d}. \quad (1)$$

$f(\alpha, d)$ is composed of two components, namely, the thickness and the intensity components.

Both terms are weighted according to their desired relative contribution. In Eq. (1), ω_{θ} and ω_I are the respective weighting factors. Both terms are normalized by their respective ranges of value per image to a unitless scale with values within [0, 1] in order allow for the two components of initially different units to be linearly combined.

The thickness component is the average of the bone thickness measured at all screw sites within one region and can be written as

$$\theta_{r \in R} = \frac{1}{N_r} \sum_{i=1}^{N_r} \tilde{T}_{r,i}, \quad (2)$$

where N_r is the number of screws in one particular region and \tilde{T} the normalized local bone thickness.

1
2 Similarly, the intensity component is the mean of the intensity values sampled along all
3
4 screws within one region, or equivalently
5
6
7

$$I_{r \in R} = \frac{1}{N_r} \sum_{i=1}^{N_r} \left[\frac{1}{n} \sum_{j=1}^n \tilde{H}_j \right]_{r,i}, \quad (3)$$

8
9
10
11
12
13
14
15 where n is the number of sampled voxels for every screw, and \tilde{H} the normalized individual
16
17 voxel intensity. The normalization step has an additional benefit, that is to circumvent the
18
19 uncalibrated images and the different scanning and machine settings.
20
21
22
23
24

25 Calculating Eq. (1) for all images results in a vector of length equal to the total number of
26
27 images p for every combination of α and d . The final objective function to be maximized is
28
29 but the magnitude of the obtained vectors. A traceable extensive search was used, thus
30
31 eliminating the need for an optimization strategy such as gradient-based approaches. A
32
33 formal representation of the total objective function is given as
34
35
36
37
38
39

$$\begin{aligned} f(\alpha, d)_{total} &= \sqrt{\sum_{im=1}^p [f(\alpha, d)_{im}]^2} \\ &= \sqrt{\sum_{im=1}^p \left[\omega_\theta \sum_{r \in R} \theta_r^{\alpha, d} + \omega_I \sum_{r \in R} I_r^{\alpha, d} \right]^2}. \end{aligned} \quad (4)$$

40
41
42
43
44
45
46
47
48
49
50
51
52
53
54
55 **HERE GOES FIGURE 3**
56
57
58

59
60
61
62
63
64
65 **HERE GOES TABLE 2**

Application, Evaluation, and Results

1
2 The first step was to measure the mandibular angle in the population using the approach
3
4 described above. The distributions of the measured gonial angles for each gender population
5
6 are listed in Table 1. The angles of female mandibles are found to be larger than those of the
7
8 males with a statistically significant difference. This result was obtained using both ANOVA
9
10 and t-test.¹⁹ These findings were used to initialize and set the domain of the optimization
11
12 along the angle parameter. We chose that value to be two standard deviations around the
13
14 mean mandibular angle of the population with steps of one degree. This choice was based on
15
16 the assumption that the measured data follow a Gaussian distribution, which was proven
17
18 through the Lilliefors test of normality.²⁰ We constrained the distance between the screws by
19
20 the screw hole geometry (6mm) and an arbitrarily larger value (16mm) with 1mm steps.
21
22 Since we did not have prior knowledge about the adequate weighting factors, we varied them
23
24 to cover all possible combinations and repeated the computations for every pair (ω_θ, ω_l). The
25
26 outcome of the optimization process was constant for $\omega_\theta \geq 0.5$ (i.e., $\omega_l \leq 0.5$) in the case of
27
28 males, and $\omega_\theta \geq 0.2$ (i.e., $\omega_l \leq 0.8$) for females. These combinations are consistent with our
29
30 design strategy to assign higher importance to the available thickness of the cortical bone.
31
32 Varying the weighting factors allows for the designer to find the optimal combination for the
33
34 specific implant and population under scrutiny. The computation time is in the range of few
35
36 milliseconds per image. However, the main processing time is occupied by the loading and
37
38 unloading of the images into memory.
39
40
41
42
43
44
45
46
47
48
49
50

51 We applied the optimization algorithm with the corresponding pair of optimal weighting
52
53 factors on each population. Eq. (4) reached its maximum value for $\alpha = 121^\circ$ and $d = 10mm$
54
55 for males and $\alpha = 129^\circ$ and $d = 9mm$ for females. The objective function is plotted in Fig. 3
56
57 against the 2D space of the design parameters.
58
59
60
61
62
63
64
65

1
2 In order to evaluate the new design, we generated implant configurations with the obtained
3 parameters and compared it with that generated using the parameters of the commercially
4 available design (low-profile MODUS[®] TriLock[®] 2.0/2.3/2.5, Medartis AG, Basel,
5 Switzerland. $\alpha = 120^\circ$ and $d = 9mm$). We applied the same method in both cases and
6 measured the resulting distribution of bone thickness along the screw insertion paths. We
7 carried out two-tailed t-tests to calculate the statistical significance of the differences in the
8 obtained results using a significance level of 0.05.¹⁹ The results are listed in detail in Table 2.
9 A graphical comparison of the geometries of the standard design and the designs proposed
10 using the method presented herein is shown in Fig. 4.
11
12
13
14
15
16
17
18
19
20
21
22
23
24
25
26
27
28
29
30

HERE GOES FIGURE 4

Discussion

31
32
33 In this paper we presented a new population-based orthopedic implant design methodology
34 that combines shape and bone quality information into a single optimization process. The
35 method was presented for the case of mandibular internal reconstruction plates. Of interest to
36 the design were two parameters, namely the angle of the plate and the distance separating two
37 consecutive screw holes. Using computational anatomy and image analysis techniques, the
38 mandibular angle and the bone thickness and intensity values at screw paths were measured.
39 This allowed us to formulate an optimization strategy to minimize the required intra-
40 operative in-plane plate bending and maximize bone quality in and around the volumes that
41 will be occupied by the screws. These two factors are to a large extent responsible for the
42 success of the fixation.^{2,10,13} We presented an evaluation of the proposed design by means of
43 a comparison with a commercially available fixator. We used a larger database of CT images
44
45
46
47
48
49
50
51
52
53
54
55
56
57
58
59
60
61
62
63
64
65

1 with higher resolution than that used in our previous study.¹⁴ The image registration
2 algorithm¹⁸ that we used for pre-processing the data was specifically design for mandibles
3 and associated implant design.
4
5
6
7
8

9 We postulated that there is a significant morphological difference between the two genders.
10 To test this hypothesis, we divided our image database into two populations of opposite
11 sexes. We measured the mandibular angle of every subject in each one of the populations of
12 available CT images. We obtained a noticeable difference between the gonial angles of male
13 and those of female subjects. This is consistent with the fact that males have sharper
14 mandibular angle than females, a sexual dimorphism that has been reported by a number of
15 studies.^{15,16,17}
16
17
18
19
20
21
22
23
24
25
26
27
28

29 The difference between the measured gonial angle and that of the standard plate indicates that
30 the latter is not optimal and has room for improvement. We used the methodology developed
31 above to propose enhanced gender-specific plate designs. The proposed and the standard
32 designs were compared in terms of available bone thickness and bone quality at screw
33 locations. A statistically significant increase was measured for the new design in the bone
34 thickness at screw insertion sites in the region of the mandibular body (males) and ramus
35 (females). Statistically non-significant improvements were observed in the remaining regions
36 for both bone thickness and intensity values at screw paths. In the cases of slight decrease in
37 the sampled intensity values (male, ramus and body), the statistical significance of the
38 changes was very low. As expected, and since the screws of the mandibular angle were fixed,
39 no change was observed in that region.
40
41
42
43
44
45
46
47
48
49
50
51
52
53
54
55
56
57
58
59
60
61
62
63
64
65

1 The proposed designs proved through computational experiments that they are capable of
2 performing better for a larger population span than the current commercial design. Within the
3 population, there is a higher probability that the proposed implants cover areas of thicker
4 cortical bone without compromising the bone mineral density around the screws. Though no
5 clinical trials have been carried out yet, experiments using medical image analysis and
6 computational anatomy methods allowed us to conclude that our design is methodologically
7 sound and that statistically a plate with angle and screw separation of 129° and 9mm for
8 females and 121° and 10mm for males are more suitable designs than the generic 120° and
9 9mm.
10
11
12
13
14
15
16
17
18
19
20
21
22
23

24 The method presented herein can be extended to be applied on other implant types and for
25 various anatomical sites. The length of the implant is not as important as its shape since in
26 practice and according to the guidelines of the AO foundation, a plate longer than needed is
27 intra-operatively cut to size. Therefore the length of the fixator was excluded from our
28 analysis. The overall length of the plate will increase with increasing distance between the
29 screw holes. Therefore, the respective effects will be correlated and redundant. We are aware
30 that the length of the fixation and the location of the screws have a direct effect on the
31 mechanical properties of the reconstruction and the force distribution over the locking
32 mechanism. However, we have set plans to closely examine this topic in a study involving
33 mechanical and finite element analysis that are outside the scope of and complement this
34 paper. We plan to compare the mechanical behavior of the standard and the proposed designs
35 in situ, in terms of distribution of forces and stresses, and resistance to screw pullout. This
36 could also be followed by clinical trials where the design method the mechanical simulations
37 and tests can be validated in the operating theatre.
38
39
40
41
42
43
44
45
46
47
48
49
50
51
52
53
54
55
56
57
58
59
60
61
62
63
64
65

Acknowledgment

This work was carried out within the frame of the National Center of Competence in Research, Computer-Aided and Image-Guided Medical Interventions (NCCR Co-Me), supported by the funds of the Swiss National Science Foundation (SNSF).

References

1. Nagamune, K., Y. Kokubo, and H. Baba. Computer-assisted designing system for fixation plate. *IEEE International Conference on Fuzzy Systems – FUZZ IEEE 2009*, pp. 975-980.
2. Frankle, M.A., J. Cordey, M.D. Frankle, F. Baumgart, S. Perren. A retrospective analysis of plate contouring in the tibia using the conventional 4.5 (narrow) dynamic compression plate. *J Orthop Trauma* 8:59–63, 1994.
3. Perren, S.M.: Evolution and rationale of locked internal fixator technology. Introductory remarks. *Injury* 32(suppl.2):B3–B9, 2001.
4. Schmutz, B., M. E. Wullschleger, H. Noser, M. Barry, J. Meek, and M. a Schutz. Fit optimisation of a distal medial tibia plate. *Comput Meth Biomech Biomed Eng* 14:359-64, 2011.
5. Wagner, M. General principles for the clinical use of the LCP. *Injury* 34(suppl. 2):B31–B42, 2003.
6. Goyal, K.S., A.S. Skalak, R.E. Marcus, H.A. Vallier, D.R. Cooperman. Analysis of anatomic periarticular tibial plate fit on normal adults. *Clin Orthop Relat Res* 461:245–257, 2007.
7. Taljanovic, M.S., M.D. Jones, J.T. Ruth, J.B. Benjamin, J.E. Sheppard, T.B. Hunter. Fracture fixation. *Radiographics* 23:1569–1590, 2003.
8. Bou-Sleiman, H., L. E. Ritacco, L.-P. Nolte, and M. Reyes. Minimization of intra-operative shaping of orthopaedic fixation plates: a population-based design. In: *Proc. 14th Int*

1
2
3
4
5
6
7
8
9
10
11
12
13
14
15
16
17
18
19
20
21
22
23
24
25
26
27
28
29
30
31
32
33
34
35
36
37
38
39
40
41
42
43
44
45
46
47
48
49
50
51
52
53
54
55
56
57
58
59
60
61
62
63
64
65

Conference on Medical Image Computing and Computer-Assisted Intervention – MICCAI 2011, Part II, pp. 409-416.

9. Kozic, N., S. Weber, P. Büchler, C. Lutz, N. Reimers, M. Á. González, and M. Reyes. Optimisation of orthopaedic implant design using statistical shape space analysis based on level sets. *Med Image Anal* 14:265-275, 2010.

10. Schiuma, D., S. Brianza, and a E. Tami. Development of a novel method for surgical implant design optimization through noninvasive assessment of local bone properties. *Med Eng & Phys* 33:256-62, 2011.

11. Merheb, J., N. Van Assche, W. Coucke, R. Jacobs, I. Naert, and M. Quirynen. Relationship between cortical bone thickness or computerized tomography-derived bone density values and implant stability. *Clin Oral Implants Res* 21:612-7, 2010.

12. Zhang, J., C.-hwang Yan, C.-kong Chui, and S. H. Ong. Accurate measurement of bone mineral density using clinical CT imaging with single energy beam spectral intensity correction. *IEEE Trans Med Imaging* 29:1382-1389, 2010.

13. Hong, J., Y.-J. Lim, and S.-O. Park. Quantitative biomechanical analysis of the influence of the cortical bone and implant length on primary stability. *Clin Oral Implants Res*, 2011.

14. Bousleiman, H., C. Seiler, T. Iizuka, L.-P. Nolte, and M. Reyes. Population-based design of mandibular plates based on bone quality and morphology. In: Proc. 15th Int Conference on Medical Image Computing and Computer-Assisted Intervention – MICCAI 2012, in press.

15. Franklin, D., P. O’Higgins, C. E. Oxnard, and I. Dadour. Sexual dimorphism and population variation in the adult mandible forensic applications of geometric morphometrics. *Forensic Science, Medicine, and Pathology* 3:15-22, 2007.

16. Oetlél, A. C., P. J. Becker, E. de Villiers, and M. Steyn. The influence of age, sex, population group, and dentition on the mandibular angle as measured on a South African sample. *Am J Phys Anthropol* 139:505-11, 2009.

- 1
2
3
4
5
6
7
8
9
10
11
12
13
14
15
16
17
18
19
20
21
22
23
24
25
26
27
28
29
30
31
32
33
34
35
36
37
38
39
40
41
42
43
44
45
46
47
48
49
50
51
52
53
54
55
56
57
58
59
60
61
62
63
64
65
17. Ponyi, S. and G. Szabó. Statistical investigation of mandibular dimensions for the planning of a series of mandibular corpus replacements. *J Craniofac Surg* 2:1049-2275, 1990.
18. Seiler, C., X. Pennec, and M. Reyes. Geometry-aware multiscale image registration via OBBTree-based polyaffine log-demons. In: Proc. 14th Int Conference on Medical Image Computing and Computer-Assisted Intervention – MICCAI 2011, Part II, pp. 631-638.
19. Petrie, A. Statistics in orthopaedic papers. *J Bone Joint Surg Br* 88:1121-36, 2006.
20. Lilliefors, H. W. On the Kolmogorov-Smirnov Test for normality with mean and variance unknown. *Journal of the American Statistical Association* 62:399-402, 1967.

Table 1. Distribution of subject age and measured mandibular angle within the gender-specific populations. The angle of the standard commercially available plate is also listed.

		Male	Female	
Count		41	39	
Age (years)	<i>Mean</i>	61.7	68.1	
	<i>Median</i>	65	71	
	<i>Std. Dev.</i>	14.6	15.3	Angle of
				Standard Plate
Angle (Degrees)	<i>Mean</i>	119.5	126.0	120.0
	<i>Median</i>	118.3	125.7	
	<i>Std. Dev.</i>	3.0	4.0	
		<i>Stat. Sig.</i>		
		$p < 0.001$	***	
		<i>Male vs. Female</i>		

Table 2. Comparison of the measured bone thickness and sampled intensity values at screw insertion sites for the standard and the proposed plate designs. The results are grouped by gender and by anatomical region (*n.s.*: not significant, μ : mean, σ : standard deviation).

		Standard		Proposed		Impr.	Stat. Sig.	<i>p</i> -val.
Male		μ	σ	μ	σ			
Thickness (mm)	<i>Ramus</i>	5.2	1.4	5.3	1.5	2 %	<i>n.s.</i>	0.08
	<i>Angle</i>	5.7	1.8	5.7	1.2	0 %	<i>n.s.</i>	1
	<i>Body</i>	9.2	2.3	9.6	2.1	4.3 %	***	<0.001
Intensity (HU)	<i>Ramus</i>	579	228	571	226	-1.4 %	<i>n.s.</i>	0.19
	<i>Angle</i>	722	193	722	193	0 %	<i>n.s.</i>	1
	<i>Body</i>	696	289	694	286	-0.3 %	<i>n.s.</i>	0.59
Female								
Thickness (mm)	<i>Ramus</i>	5.0	1.8	5.5	1.7	10 %	***	<0.001
	<i>Angle</i>	6.3	1.4	6.3	1.4	0 %	<i>n.s.</i>	1
	<i>Body</i>	10.7	2.1	10.7	2.1	0 %	<i>n.s.</i>	1
Intensity (HU)	<i>Ramus</i>	589	234	592	215	0.5 %	<i>n.s.</i>	0.79
	<i>Angle</i>	634	247	634	247	0 %	<i>n.s.</i>	1
	<i>Body</i>	635	230	635	230	0 %	<i>n.s.</i>	1

Figure 1. 3D view of the reference mandible with the standard fixation plate placed in its correct location. (A) Visible landmarks (red circles) used to measure the mandibular angle. (B) Anatomical grouping of the mandible and plate into three regions, namely, ramus, angle, and body of the mandible. (C) Illustration of the in-plane and out-of-plane deformations relative to the plate.

1
2
3
4
5
6
7
8
9
10
11
12
13
14
15
16
17
18
19
20
21
22
23
24
25
26
27
28
29
30
31
32
33
34
35
36
37
38
39
40
41
42
43
44
45
46
47
48
49
50
51
52
53
54
55
56
57
58
59
60
61
62
63
64
65

Figure 2. Volume rendering of the reference image showing the (A) landmarks corresponding to the screw sites of a 120° and 9mm plate and (B) the paths of the screws along which the intensity values are sampled.

1
2
3
4
5
6
7
8
9
10
11
12
13
14
15
16
17
18
19
20
21
22
23
24
25
26
27
28
29
30
31
32
33
34
35
36
37
38
39
40
41
42
43
44
45
46
47
48
49
50
51
52
53
54
55
56
57
58
59
60
61
62
63
64
65

Figure 3. Surface plots of the objective function for the (*top*) male and (*bottom*) female populations against the 2-dimensional optimization space spanned by the design parameters α and d . The green circle is the peak value.

1
2
3
4
5
6
7
8
9
10
11
12
13
14
15
16
17
18
19
20
21
22
23
24
25
26
27
28
29
30
31
32
33
34
35
36
37
38
39
40
41
42
43
44
45
46
47
48
49
50
51
52
53
54
55
56
57
58
59
60
61
62
63
64
65

Figure 4. Overlay comparison of the geometries of the (*green*) standard and the proposed designs for (*blue*) males and (*red*) females.

1
2
3
4
5
6
7
8
9
10
11
12
13
14
15
16
17
18
19
20
21
22
23
24
25
26
27
28
29
30
31
32
33
34
35
36
37
38
39
40
41
42
43
44
45
46
47
48
49
50
51
52
53
54
55
56
57
58
59
60
61
62
63
64
65

Figure1
[Click here to download high resolution image](#)

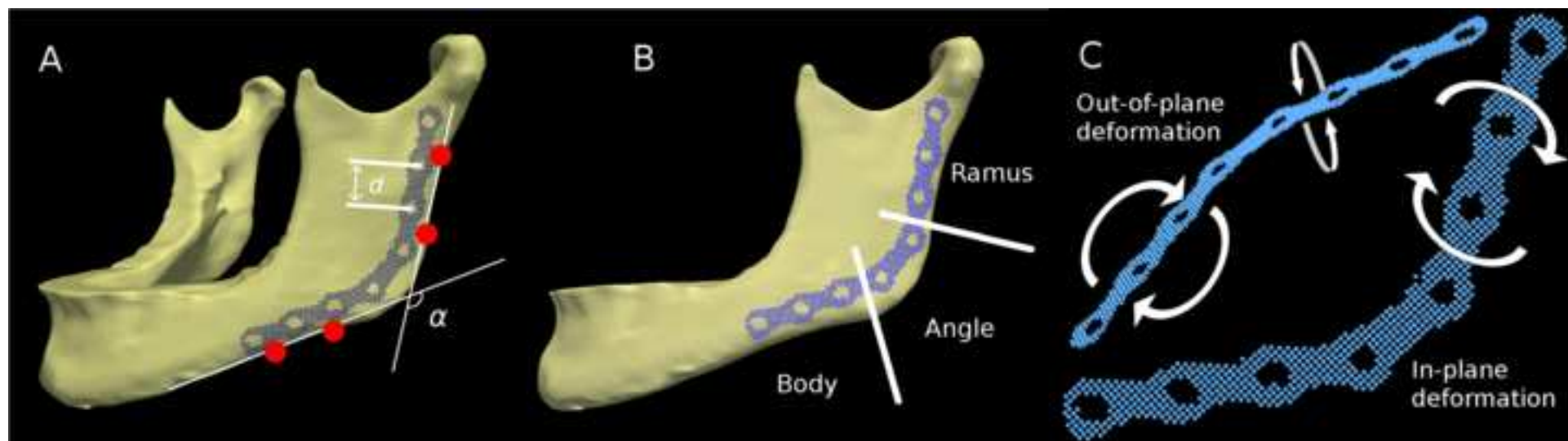


Figure 2

[Click here to download high resolution image](#)

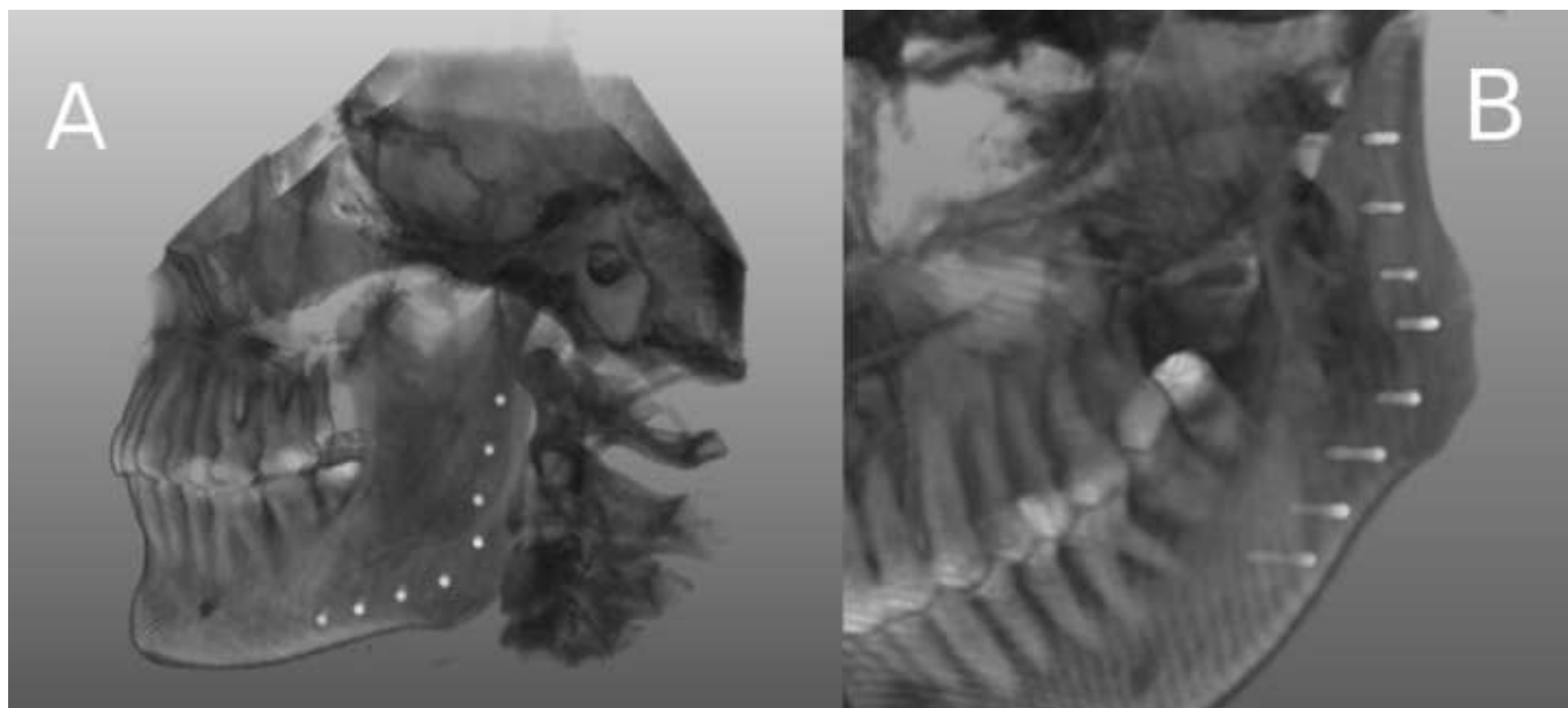


Figure3

[Click here to download high resolution image](#)

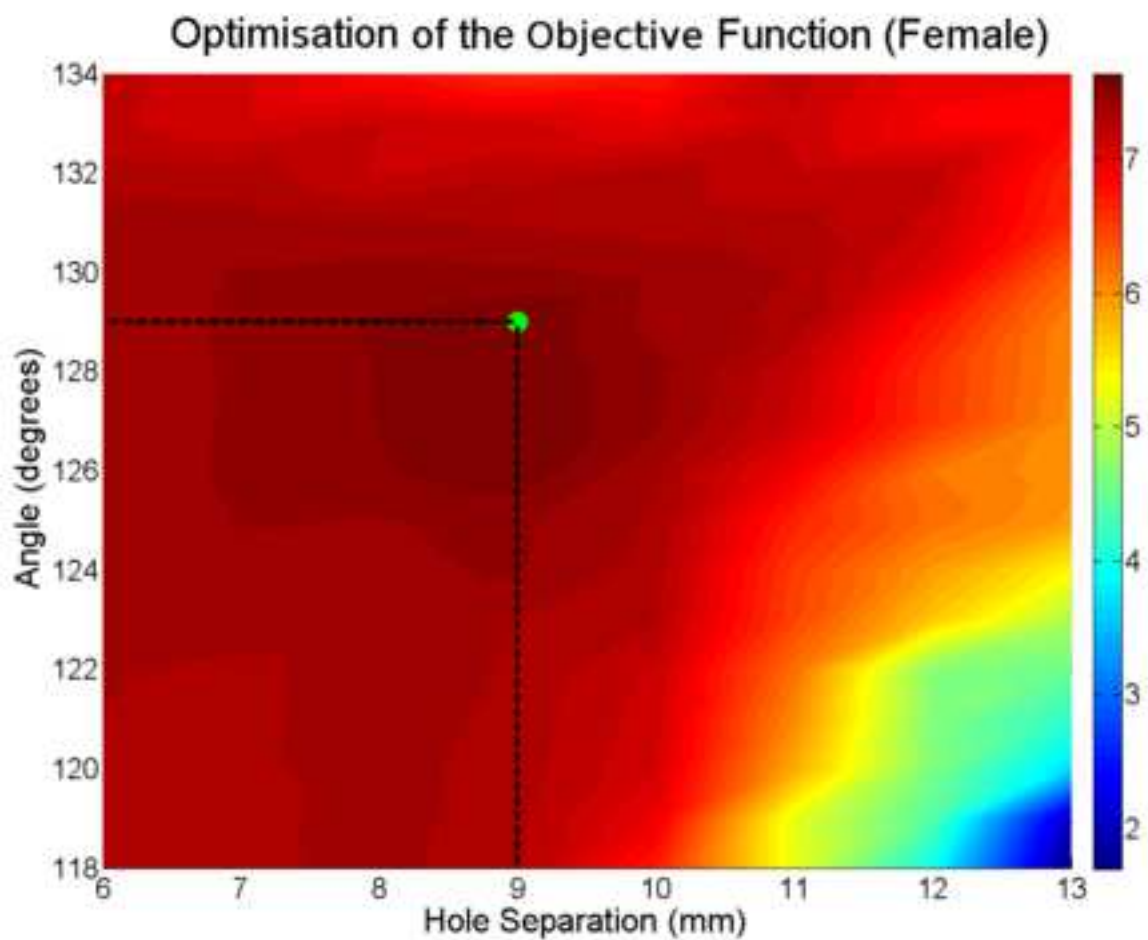
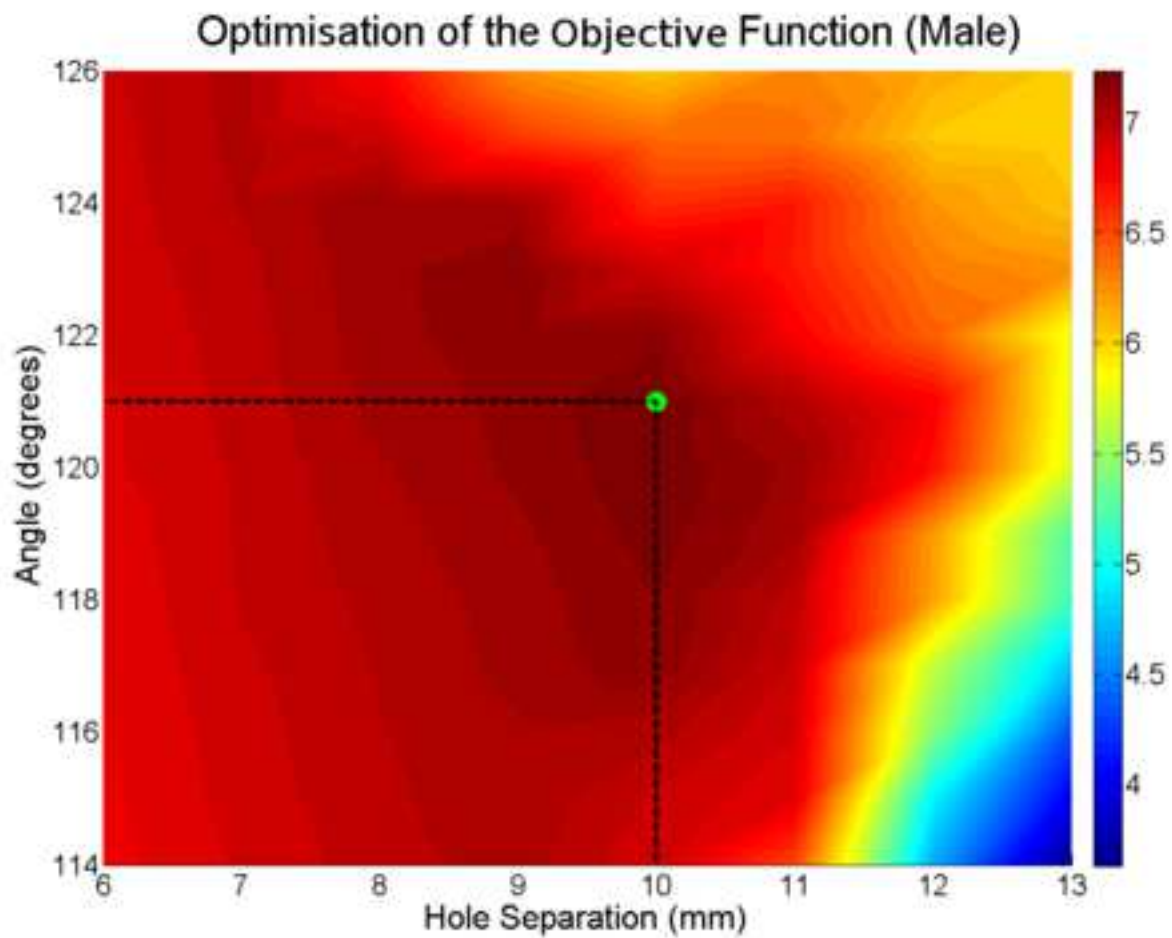
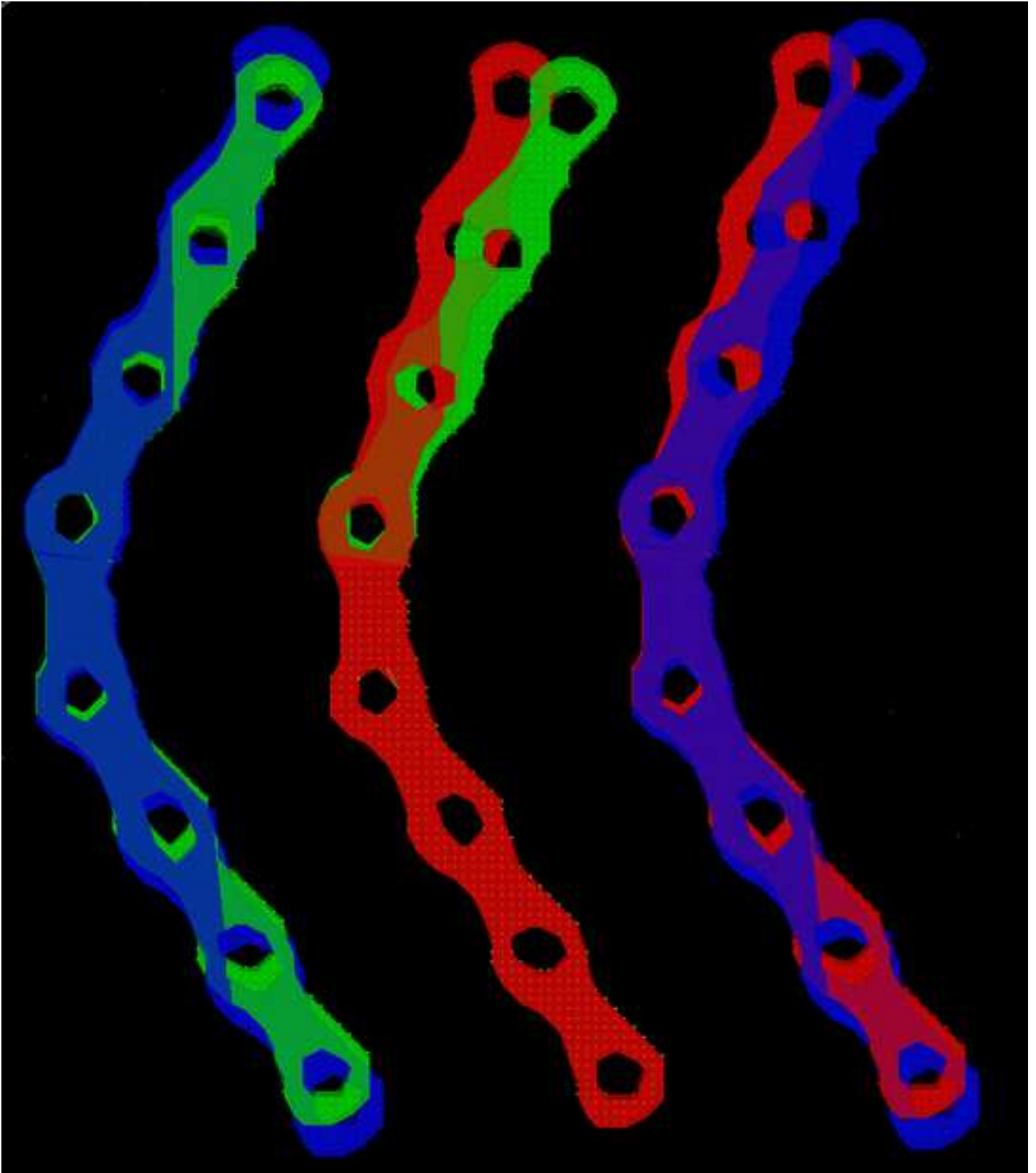


Figure4
[Click here to download high resolution image](#)



*Form for Disclosure of Potential Conflicts of Interest

[Click here to download Form for Disclosure of Potential Conflicts of Interest: coi_disclosure.pdf](#)